



Spectral Wave Characteristics in the Nearshore Waters of Northwestern Bay of Bengal

M. ANJALI NAIR,¹ V. SANIL KUMAR,¹  and M. M. AMRUTHA¹

Abstract—The spectral wave characteristics in the nearshore waters of northwestern Bay of Bengal are presented based on the buoy-measured data from February 2013 to December 2015 off Gopalpur at 15-m water depth. The mean seasonal significant wave height and mean wave period indicate that the occurrence of higher wave heights and wave periods is during the southwest monsoon period (June–September). 74% of the sea surface height variance in a year is a result of waves from 138 to 228° and 16% are from 48 to 138°. Strong inter-annual variability is observed in the monthly average wave parameters due to the occurrence of tropical cyclones. Due to the influence of the tropical cyclone Phailin, maximum significant wave height of 6.7 m is observed on 12 October 2013 and that due to tropical cyclone Hudhud whose track is 250 southwest of the study location is 5.84 m on 12 October 2014. Analysis revealed that a single tropical cyclone influenced the annual maximum significant wave height and not the annual average value which is almost same (~ 1 m) in 2014 and 2015. The waves in the northwestern Bay of Bengal are influenced by the southwest and northeast monsoons, southern ocean swells and cyclones.

Key words: Surface waves, multi-peaked spectra, wind-seas, swells, directional waves spectra, east coast of India.

1. Introduction

Sea surface is the point of interaction between the atmosphere and the ocean and the surface waves are the result of the energy transfer from atmosphere to the ocean. Surface waves are a natural hazard affecting the coastal zones resulting in damage to the coastline and control the energy impacting the coastlines and coastal defenses. The variability in wave climate has different time scales ranging from hour, day, month, season, year and decade. Hence, comprehensive understanding of the properties of the

wind generated waves and their potential changes are to be known for planning marine facilities in the ocean (Anoop et al. 2015). Although wind speed is closely related to wave heights, the spatial patterns of the two fields are not analogous due to the propagation of waves over long distances (Chen et al. 2002). The wave characteristics at a location depend on the wind speed and direction, fetch parameters, bathymetry and the deep-water wave propagation processes. Bay of Bengal (BoB) is a tropical basin with semi-annual reversal of winds due to the summer (June–September) and winter (October–January) monsoon system and the winds blow from the southwest (SW) during the summer and from the northeast (NE) during the winter monsoon (Thadathil et al. 2007). The changes in the wind pattern influence the waves in the BoB (Sanil Kumar et al. 2014). Anoop et al. (2015) reported that the wave climate of BoB shows a large response to seasons due to seasonally reversing winds. Waves in most of the oceans consist of swells propagating from far-off and the locally generated waves and result in multi-peaked wave energy spectrum (Soares 1991; Hanson and Philips 1999) and the BoB also has no exception. The wave climate of BoB is influenced by conditions in the Indian Ocean since the fetch for the predominantly southerly winds is sufficient to generate swell waves. Wave spectra characterization has gained considerable relevance in recent years as a result of increasing demand for detailed wave information. In the Indian coastal waters, the wave energy spectra contain multiple peaks for about 60% of the time in a year and the multi-peaked wave spectra observed consists of multiple swells and wind-sea and are largely dominated by swells (Sanil Kumar et al. 2003). When multiple wave systems are present at a location, the bulk wave parameters (significant wave height, mean wave period and mean wave direction)

¹ Ocean Engineering Division, CSIR-National Institute of Oceanography (Council of Scientific & Industrial Research), Dona Paula, Goa 403004, India. E-mail: sanil@nio.org

may not represent the true wave characteristics of a location (Sanil Kumar et al. 2014). In the northeastern BoB, during the SW monsoon period, the spectral peak is around 0.065–0.12 Hz (16–8 s) during 75% of the time whereas during the same period along the eastern Arabian Sea, the spectral peak varied in a narrow range (10–12 s) during 72% of the time (Sanil Kumar et al. 2014).

Annually, an average three to four storms form in the BoB (Alam et al. 2003). The primary season for the tropical cyclones (TCs) in the BoB is October–December and the secondary season is April–June (Li et al. 2013) indicating a bimodal distribution of the TCs. Many cyclonic storms cross the Odisha coast during May (pre-monsoon) and October–November (post-monsoon) (Balaguru et al. 2014). Wang et al. (2013) proposed that increasing sea surface temperature in the BoB has contributed to an increase in the pre-monsoon cyclone intensity since 1979. Balaguru et al. (2014) indicated that the intensity of TCs during post-monsoon during 1981–2010 has increased.

On the basis of the wave data collected during the SW monsoon (June–September) in 2009, Suresh et al. (2010) studied the wind-seas and swells off Visakhapatnam and found that the waves are mainly swells during SW monsoon. The wave statistical parameters during TC Phailin which crossed the northern BoB are described based on the wave data for 8–13 October 2013 by Amrutha et al. (2014) and reported that at 50-m water depth, the maximum wave height (H_{\max}) of 13.5 m is measured. Seasonal and annual wave characteristics off Gopalpur are studied by Patra et al. (2016) based on wave data collected for the years 1994, 2008–2009 and 2013–2014 and observed that the waves are predominantly from the south during the SW monsoon and south–southeast for rest of the year.

Based on the wave measurements carried out from February 2013 to December 2015 and the ERA-Interim (ERA-I) reanalysis wave data for the period 1979–2015, we describe the characteristics of waves off Gopalpur in northwestern BoB (Fig. 1). Gopalpur is located along northwestern part of the BoB, a fairly straight coastline with an orientation of 48°E to the north (Patra et al. 2016). The average tidal ranges near Gopalpur Port during spring and neap tides are 2.39 and 0.85 m, respectively (Mishra et al. 2011). The study period

covers two tropical cyclones (Phailin and Hudhud) which significantly influenced the waves off Gopalpur. The paper is organized as follows. The methodology and the datasets used in the study are described in Sect. 2. The results and discussion are given in Sect. 3 and conclusions are presented in Sect. 4.

2. Materials and Methods

In connection with the coastal wave forecast system of the Indian National Centre for Ocean Information Services, Hyderabad, a directional waverider buoy (Datawell 2009) is deployed off Gopalpur and the data collected under this program is used in the present study. The measurement location is around 15-m water depth (geographic position 19.2817°N; 84.9640°E) and the location is ~ 1.3 km from the mainland of India. Three accelerometers (one vertical and two horizontal) are present inside the waverider buoy. The data of heave and two translational motion of the buoy are sampled at 3.84 Hz. A digital high-pass filter with a cut off at 30 s is applied to the 3.84 Hz samples. At the same time, it converts the sampling rate to 1.28 Hz and stores the time series data at 1.28 Hz. From the time series data for 200 s, the wave spectrum is obtained through a fast Fourier transform (FFT). During half an hour 8 wave spectra of a 200 s data interval each are collected and averaged to get a representative wave spectrum for half an hour (Datawell 2009). The spectral analysis results in wave spectrum with a resolution of 0.005 Hz from 0.025 to 0.1 Hz and thereafter it is 0.01 Hz up to 0.58 Hz. The details of the spectral analysis applied to the time series are similar to that presented in Sanil Kumar et al. (2014). Significant wave height (H_{m0}), mean wave period (T_{m02}) and spectral peak period (T_p) is estimated from the wave spectrum. Mean wave direction (θ_m) corresponding to the spectral peak is estimated following Kuik et al. (1988). The 1-D separation method proposed by Portilla et al. (2009) is used to separate the wind-seas and swells from the measured data and is based on the assumption that, the energy at the peak frequency of a swell cannot be higher than the value of a Pierson–Moskowitz (PM) spectrum with the same frequency. If the ratio between the peak energy

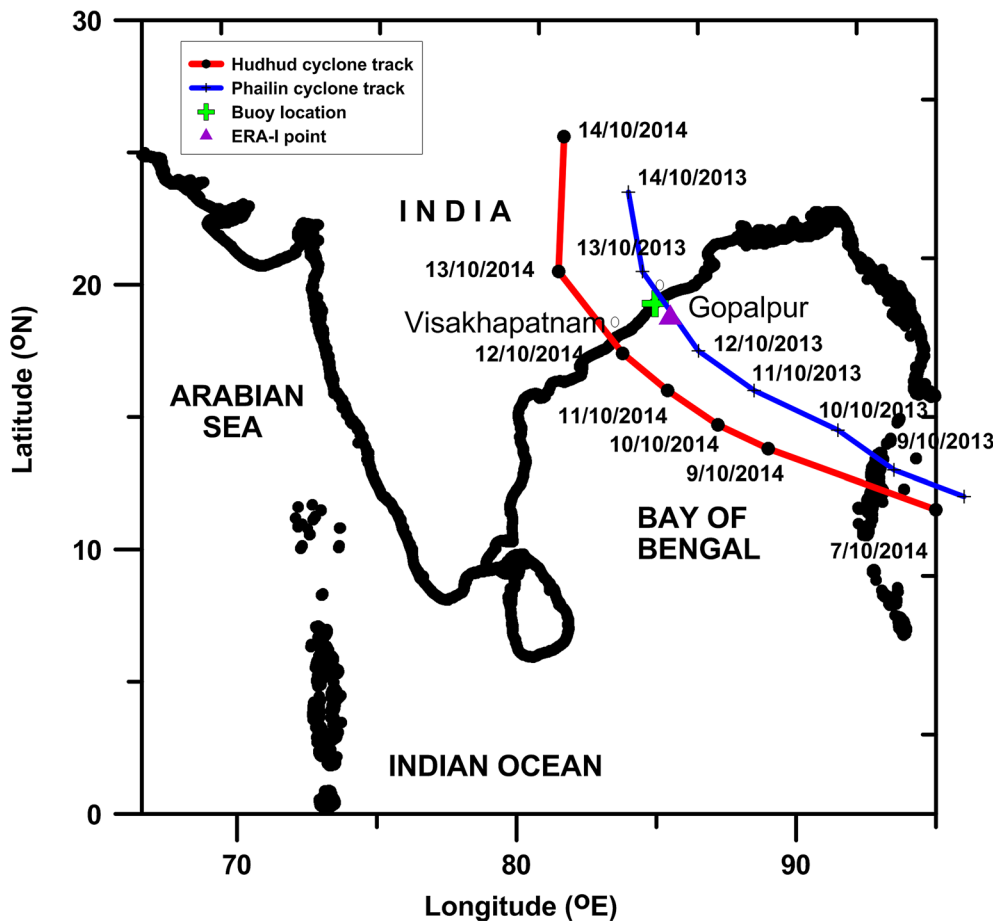


Figure 1

Location of waverider buoy in northern Bay of Bengal. The track of the tropical cyclones Phailin and Hudhud are also shown in the figure

of a wave system and the energy of a PM spectrum at the same frequency is above a threshold value of 1, the system is considered to represent wind-sea, else it is taken to be swell. A separation frequency f_c is estimated following Portilla et al. (2009) and the swell and wind-sea parameters are obtained for frequencies ranging from 0.025 Hz to f_c and from f_c to 0.58 Hz, respectively. The monthly averaged wave spectrum is estimated by averaging the wave spectrum at half-hourly interval over a calendar month. The time referred in this study is in Coordinated Universal Time (UTC). The meteorological convention is used for presenting the wind and wave direction data (0 and 360° for wind/wave from North, 90° for East, 180° for South, 270° for West). To study the inter-annual variations, the ERA-I data (Dee et al.

2011) for grid point 18.75°N; 85.50°E from European Centre for Medium-Range Weather Forecasts (ECMWF) is used. ERA-I has a temporal resolution of 6 h and spatial resolution of 0.75°.

3. Results and Discussion

3.1. Bulk Wave Parameters

The wave characteristics at a location are generally presented through significant wave height and mean wave period. For the study area, the annual average significant wave height during 2014 and during 2015 is 1 m. Since the data collection started only in February 2013, the annual average H_{m0} during 2013 is not presented. 53.7% of the time in a

year, H_{m0} is < 1 m and is similar to the wave characteristics off Visakhapatnam which is 250 km southwest of the present measurement location (Sanil Kumar et al. 2014). During 2013 and 2014, the study area was influenced by TC Phailin and TC Hudhud and hence annual maximum H_{m0} of 6.7 and 5.8 m was measured in October 2013 and October 2014, respectively. The annual maximum H_{m0} in 2015 is only 3.2 m measured during the southwest monsoon period and is similar to the value (3.3 m) observed in 2008 by Patra et al. (2016) for Gopalpur. Earlier studies show that off Gopalpur in 1990, maximum H_{m0} of only 2.4 m was measured (Chandramohan et al. 1993). Cyclonic storm Hudhud originated from a low-pressure system that formed under the influence of an upper-air cyclonic circulation in the south Andaman Sea on 6 October 2014 intensified into a cyclonic storm on 8 October and as a severe cyclonic storm on 9 October (Harikumar et al. 2016). Severe cyclonic storm Hudhud made landfall about 30 km west-northwest of Visakhapatnam on October 12, noon local time and the maximum sustained wind speeds were 115 knots (Joint Typhoon Warning Center) corresponding to a weak Category 4 hurricane on the Saffir–Simpson Hurricane wind scale. Even though the track of TC Hudhud was ~ 200 km southwest of the wave measurement location of Gopalpur, a maximum H_{m0} of 5.8 m and a maximum wave height (H_{max}) of 9.2 m was observed on 12 October 2014 due to the influence of TC Hudhud. Due to the influence of the TC, H_{m0} increased from 1 to 5 m during 9 October 2014 07 h to 12 October 2014 05 h and peak wave period shifted from 14 to 12 s [peak frequency shifted from low (~ 0.075 Hz) to high (~ 0.08 Hz)]. By 23 h on 15 October 2014, the sea state becomes normal with H_{m0} around 1 m. Due to the influence of TC Phailin, maximum H_{m0} measured at 15-m water depth was 6.7 m (Amrutha et al. 2014), which is much higher than the maximum H_{m0} during the TC Hudhud since the distance of TC Phailin from buoy location was only ~ 50 km, whereas that of TC Hudhud is ~ 200 km.

ERA-I data during 1979 to 2015 are used to study the spatial variation of mean H_{m0} , in the BoB during different seasons (Fig. 2). In the central BoB, the mean H_{m0} is found to be highest (~ 2 to 2.5 m) during the southwest monsoon period and the annual

average H_{m0} in the coastal region is less than 1.5 m. During the pre-monsoon (February–May) and post-monsoon (October–January) seasons, the mean H_{m0} is between 1 and 1.5 m and during all the seasons, the mean H_{m0} is high for southerly waves, since waves generated in the south Indian Ocean and Southern Ocean approach from the southerly direction (Chena et al. 2002; Glejin et al. 2013; Amrutha et al. 2017).

Comparison of time series plots of H_{m0} and energy period of ERA-I with measured buoy data during 3 years are shown in Fig. 3. H_{m0} obtained from ERA-I data shows a good correlation with the measured H_{m0} for $H_{m0} < 2.5$ m. The larger waves are underestimated in ERA-I. Significant wave height shows higher value during the southwest monsoon period and the two specific peaks are obtained during the TCs Phailin and Hudhud. The ERA-I data gives a comparatively good account of H_{m0} during Hudhud (measured H_{m0} value is 5.5 m and the ERA-I value is 4.6 m), whereas during Phailin, the H_{m0} by ERA-I (~ 4.1 m) is 2/3rd of the measured value (6.3 m) indicating that high waves are largely underestimated in ERA-I due to its large spatial and temporal resolution. In addition, due to the large temporal resolution (6 h), the peak H_{m0} values are missed in ERA-I. In the case of mean wave period, most of the time, the ERA-I data overestimates the measured mean wave period (Fig. 3). The scatter plot also shows that the ERA-I H_{m0} gives a good estimate of H_{m0} with bias values ranging from 0.18 to 0.24 m, whereas energy period given by ERA-I largely underestimates the measured value with bias -0.3 to -0.7 s (Fig. 4).

The change in wave parameters over different months during the 3 years are given in Fig. 5. The inter-annual variations in H_{m0} are maximum during October with the maximum value of H_{m0} in 2013 (Fig. 5a) due to the occurrence of cyclonic storms Phailin (in 2013) and Hudhud (in 2014) in October and the Phailin track was close to Gopalpur. Maximum spectral energy density observed also shows similar variations in October with the highest value in 2013 (Fig. 5d). Inter-annual variations seen in mean wave period is very less, but the peak wave period shows much variation, especially during May, June and August (Fig. 5b, c). The mean wave period during the pre-monsoon season is less and it

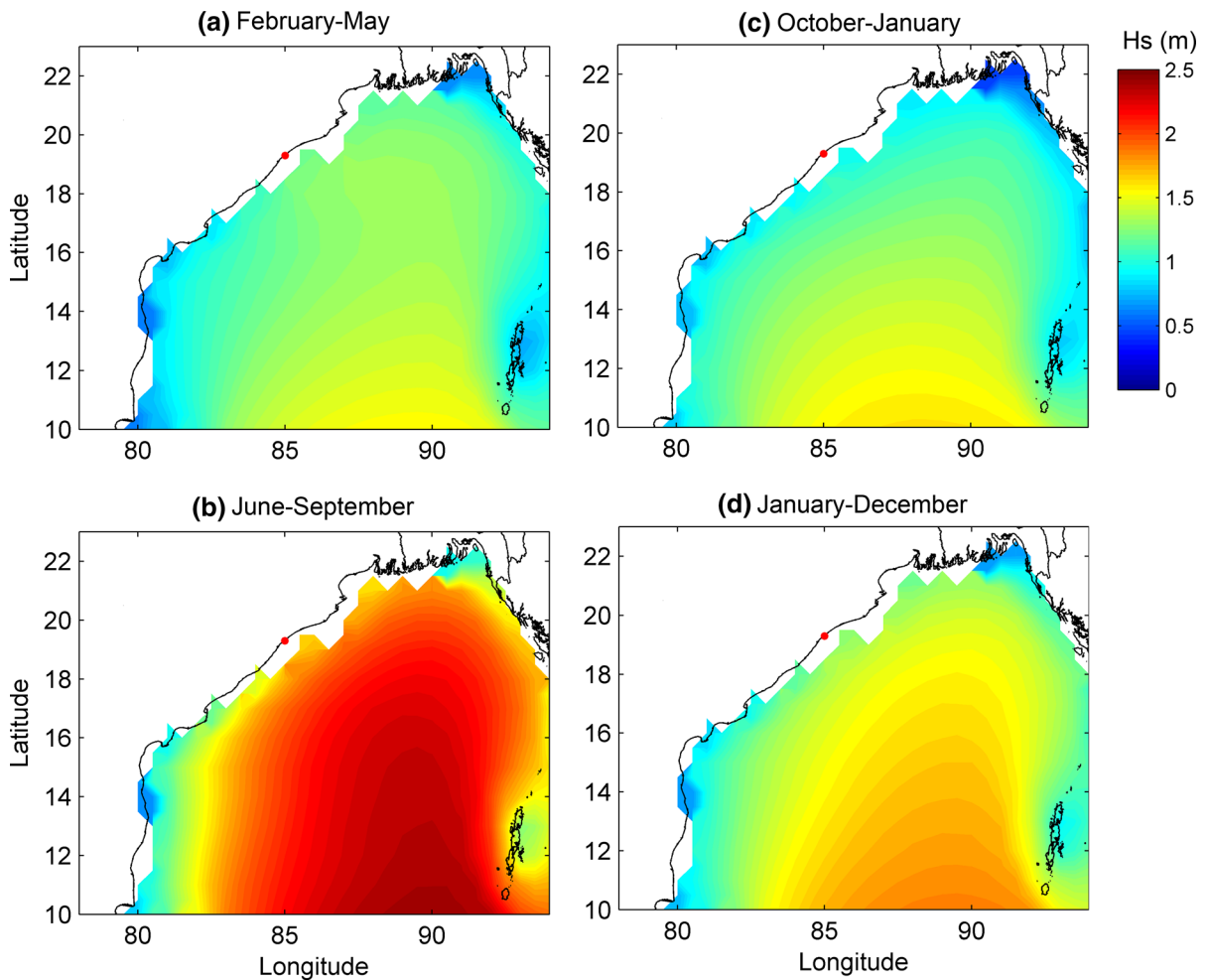


Figure 2

Mean significant wave height in Bay of Bengal during **a** February–May, **b** June–September, **c** October–January and **d** January–December. ERA-I data during 1979–2015 is used. The red dot near the coast indicates the waverider buoy location

gradually increases during southwest monsoon and reaches its maximum value during October and then decreases. Peak wave period shows its minimum values during the southwest monsoon period and it is maximum during the non-monsoon period except in 2014. The peak wave period variation in 2014 is specific with a sudden dip in wave period during July. Wave direction observed is between 150° and 170° during all the months with no significant inter-annual variations. The directional histograms for significant wave height and peak period shows the same pattern. The highest concentration of waves and the highest significant wave height values are from the quadrant

southeast. The wind-seas are originated from the direction south and east. Mishra et al. (2011) observed that waves approaching from south–southwest and east become south and east–southeast, whereas waves from the southeast continue to move in the same direction without any significant refraction in the shallow regions of Gopalpur.

To study the effect of the tropical cyclone on waves, the wave parameters during the Hudhud cyclone period are examined (Fig. 6). From the figure, it can be seen that the H_{m0} increases from 1 to 5.8 m during the TC period and the maximum H_{m0} observed is on 12 October 2014, when the cyclone

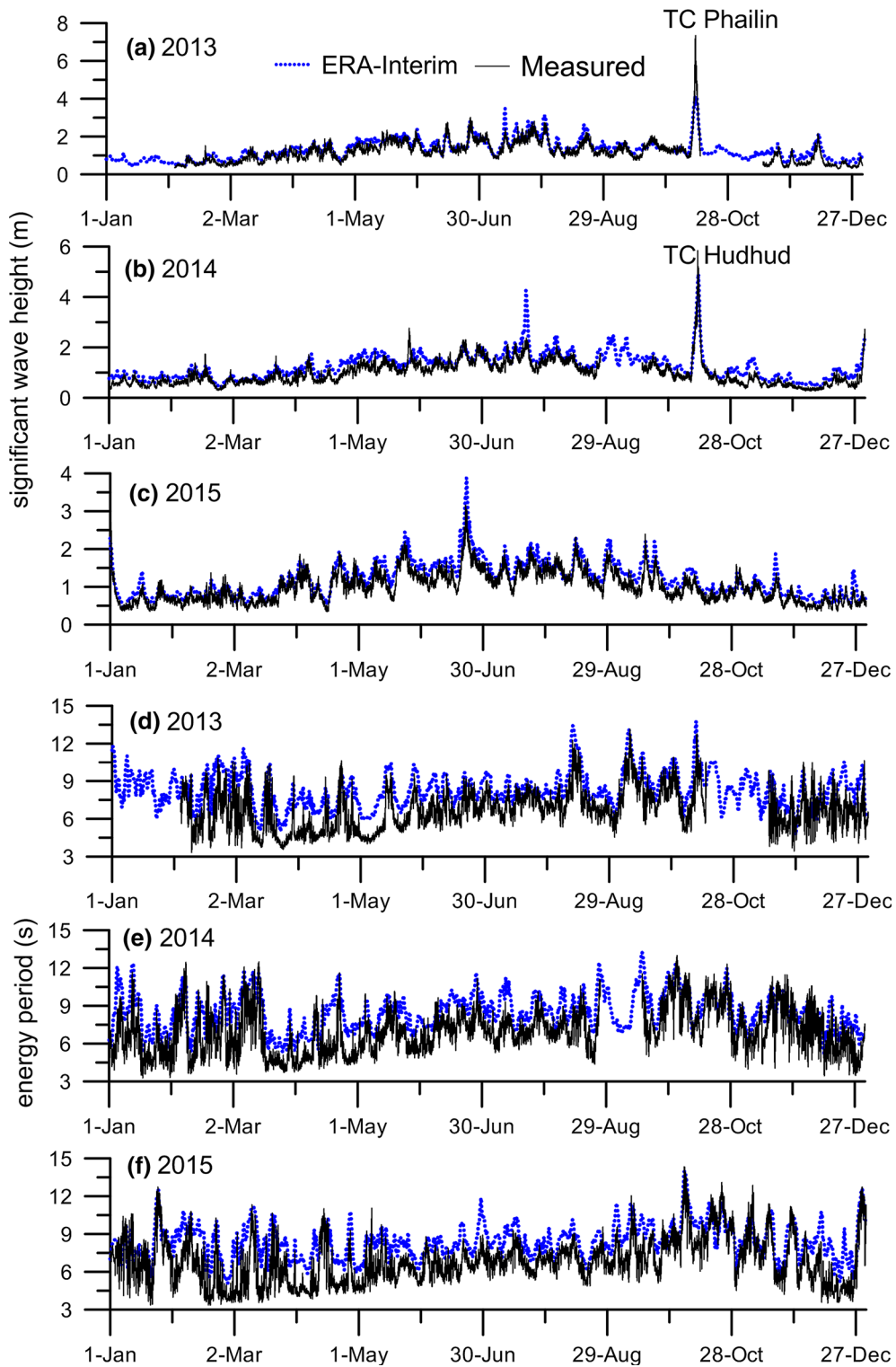


Figure 3

Time series plot of significant wave height measured (a–c) and ERA-I and mean wave period (d–f) during 2013, 2014 and 2015

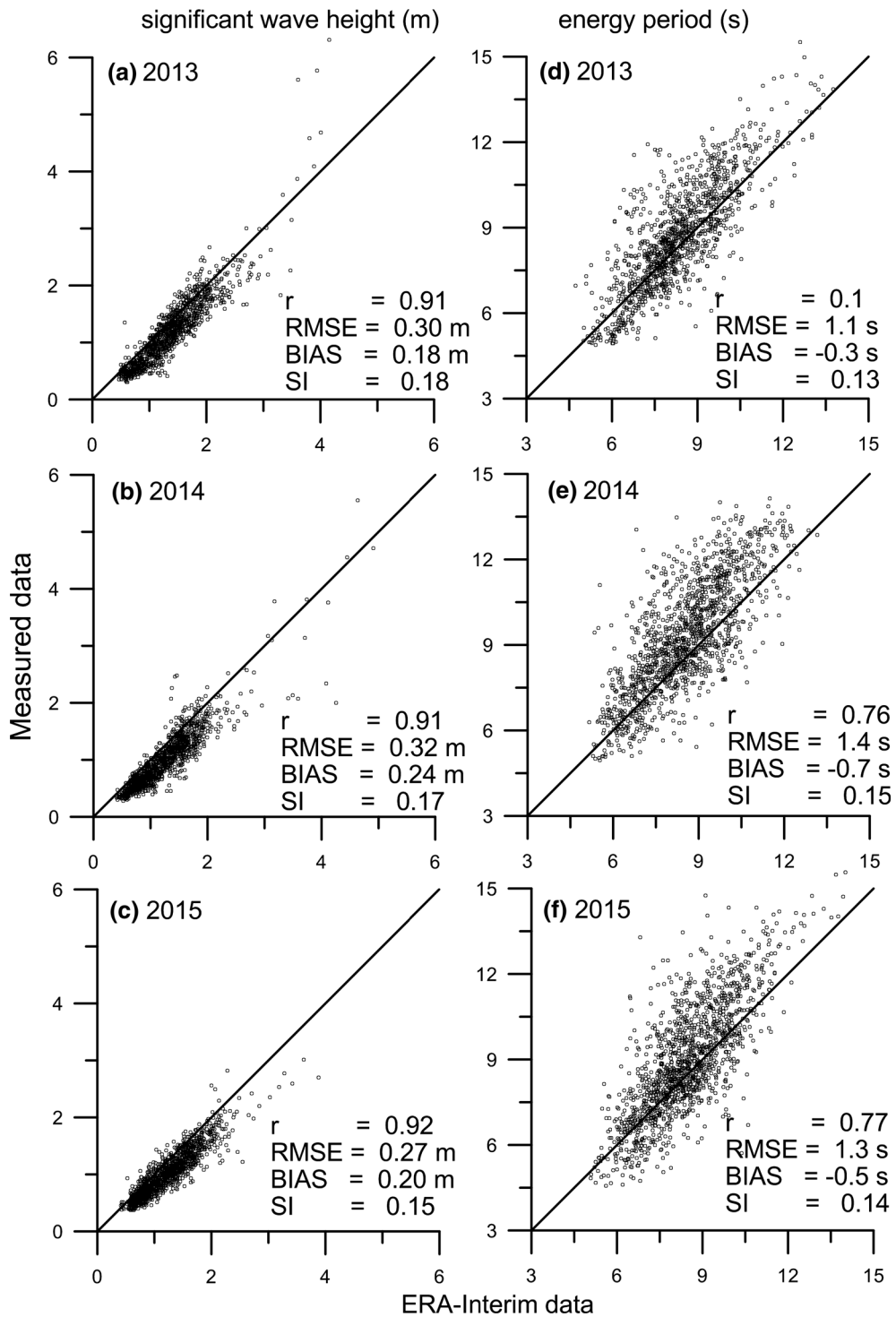


Figure 4

Scatter plot of measured significant wave height with that from ERA-I (left panel) and energy period (right panel) in different years

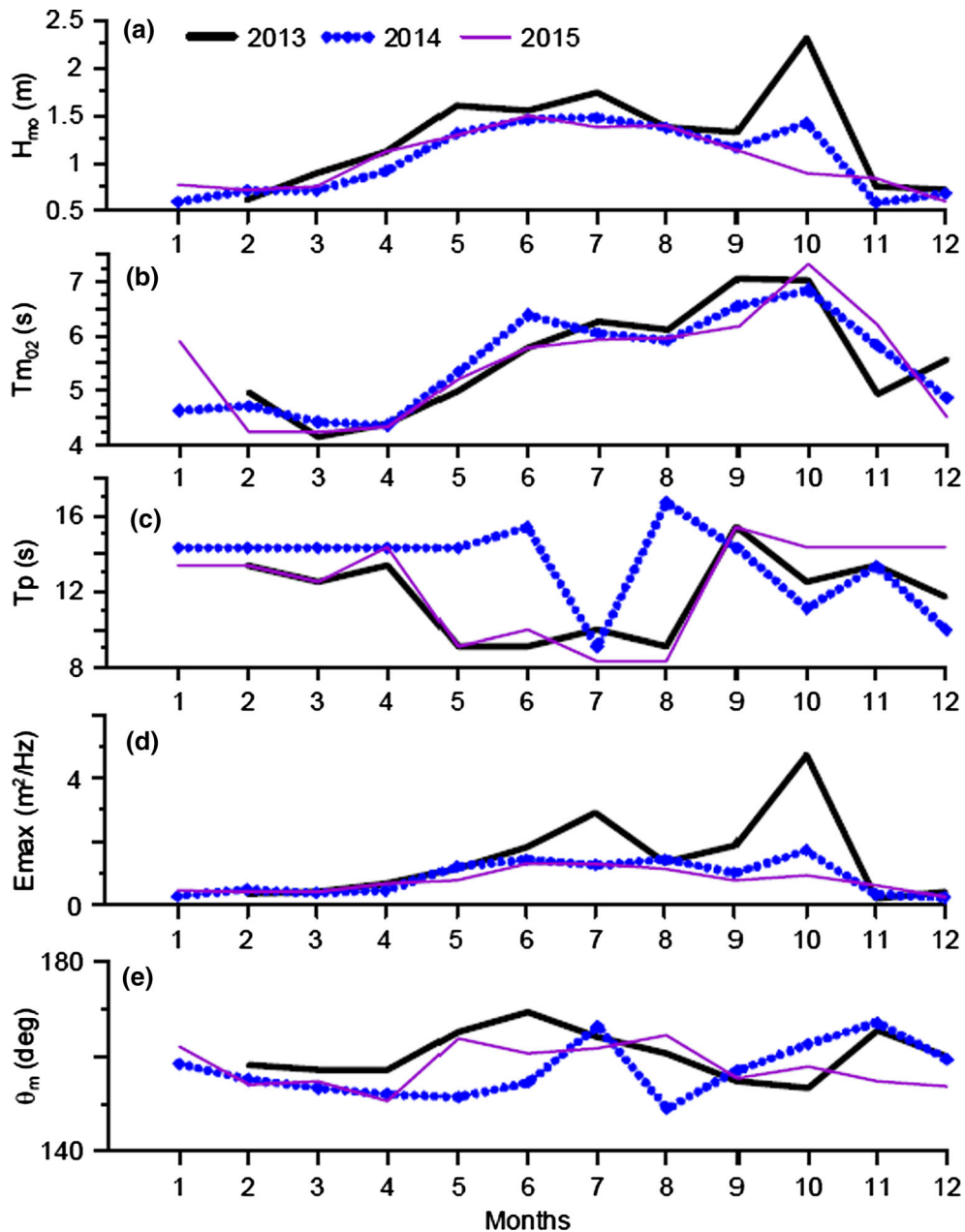


Figure 5

Wave parameters **a** significant wave height, **b** mean wave period, **c** peak wave period, **d** maximum spectral energy density and **e** mean wave direction from monthly average wave spectrum of measured data

was relatively close to the buoy location and the maximum wave height (H_{max}) observed on 12 October 2014 is 8 m (Fig. 6a). On comparing the H_{m0} of wind-seas and swells, it is found that both have its maximum values during 12 October, whereas

H_{m0} of wind-seas (3 m) is much less than that of swells (5 m) (Fig. 6b). Waves during the TC period are dominated by high energy swells (Fig. 6b). This is because the track of the cyclone is ~ 200 km southwest of location studied and hence the effect of

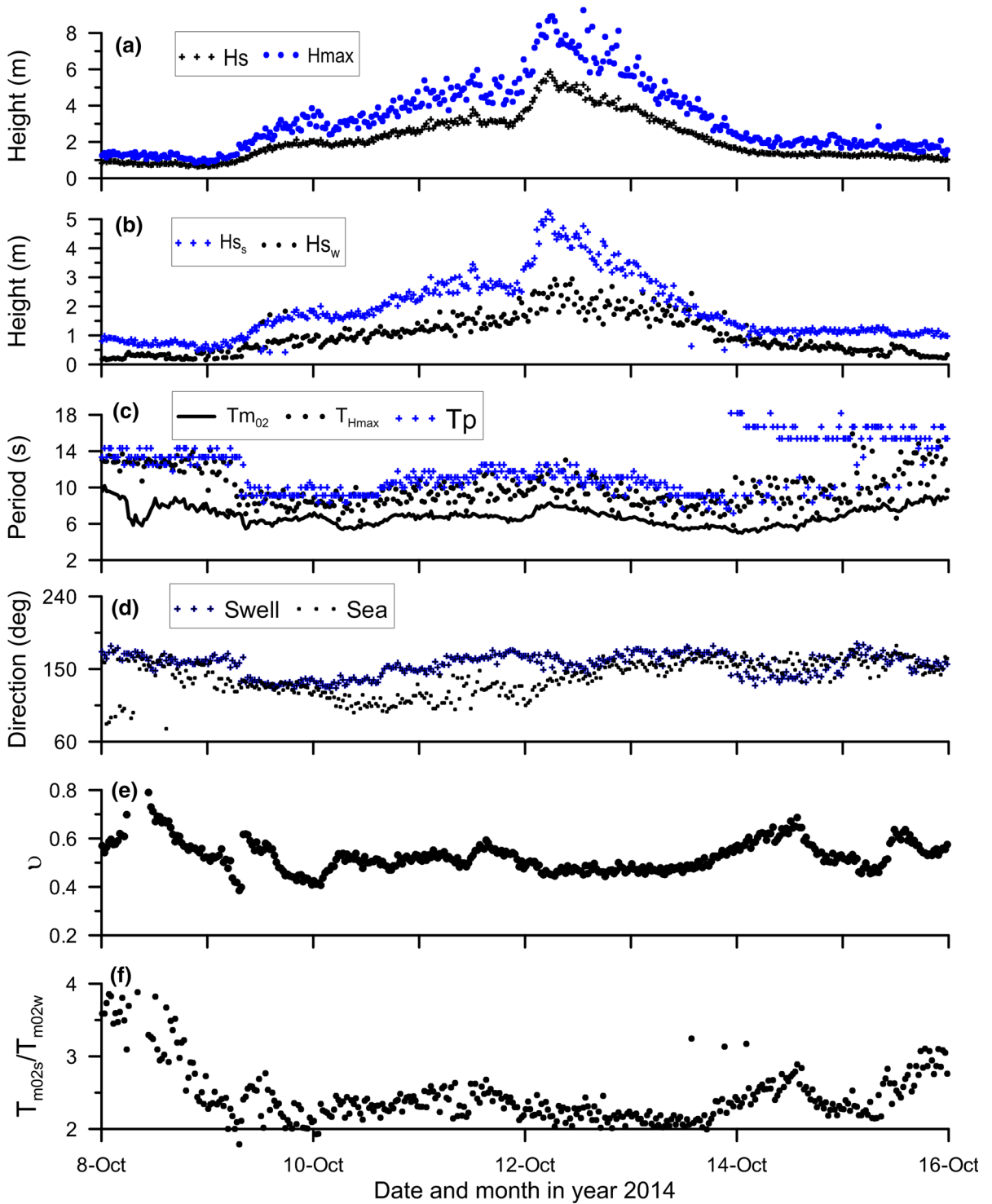
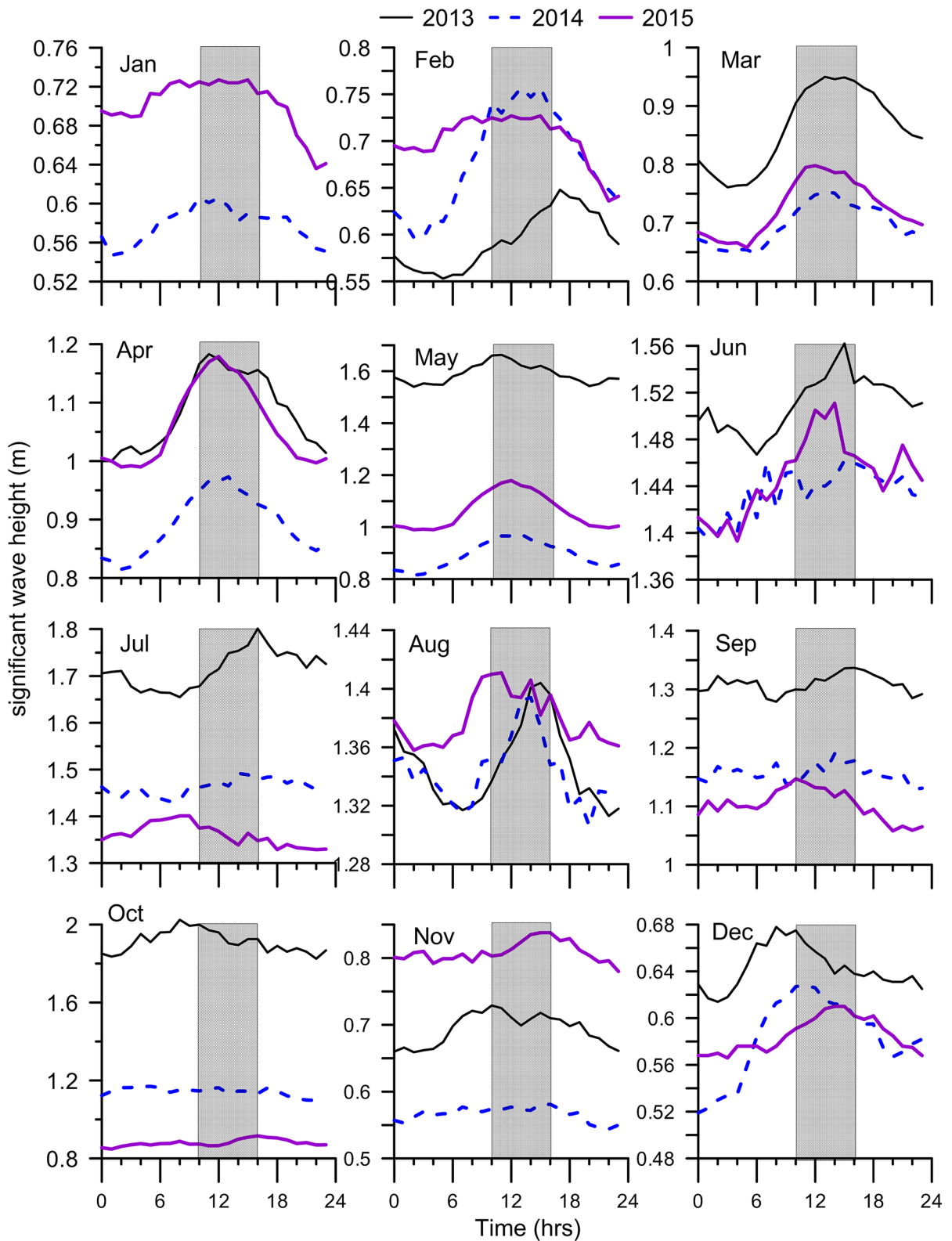


Figure 6
Plot of wave parameters during tropical cyclone Hudhud



◀Figure 7

Diurnal variation of significant wave height in different months in 2013, 2014 and 2015. The shaded area is the time during which the wave height is maximum in most of the months

the cyclonic storm on wind-seas is comparatively less. The swells which are generated near the cyclone location and propagate to reach the study location with a peak period of 12 s. The peak period observed before and after the cyclone period is 14 s (Fig. 6c). No significant variations are observed in the mean wave period during the cyclone time. The effect of cyclones on wind-seas can be identified from the wave direction. Before the cyclone, the wind-sea

direction was between 150° and 180°, but during the cyclone period, the wind-sea direction is changed to 60–150° and it shows that the wind-sea direction shifted from southeast to east (Fig. 6d). The spectral narrowness parameter changed from 0.8 to 0.5, indicating that the spectrum changed from broad to narrow during the cyclone (Fig. 6e). The ratio of mean wave period of swell and wind-seas shows that, the ratio is higher (~ 4) before the cyclone period and it gets reduced to 2.5 during the cyclone (Fig. 6f). The decrease in ratio shows that during the cyclone period, the period of swells decreases and that of wind-seas increases. This is due to the downshift of energy due to non-linear interactions, as the swells

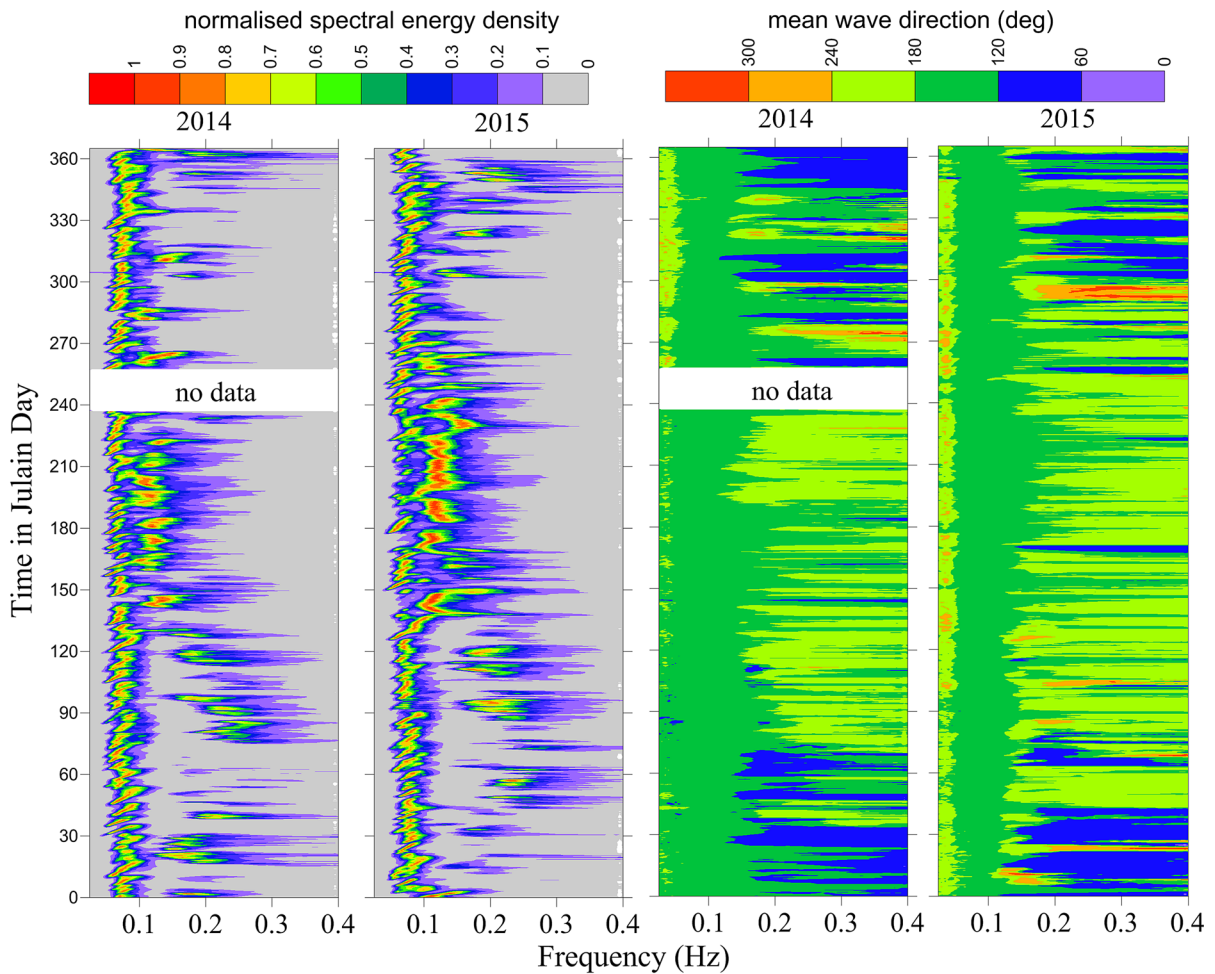


Figure 8

Left two panels shows the time series plot of the normalized spectral energy density with frequency in 2014 and 2015. Two panels in the right indicates the time series plot of wave direction with frequency

travel greater distance since the cyclone is further away.

Diurnal variations in significant wave height in different months shows that in general, the H_{m0} is low during early hours, then gradually increases and reaches its maximum during 10–16 h, then gradually decreases (Fig. 7) except in October and December 2013 and in July 2015. This is due to the impact of local sea breeze which gets activated in the late afternoon. Least diurnal variation is observed during October 2013 and 2014 is due to the influence of severe cyclonic storms which reduce the impact of local sea breeze.

3.2. Wave Spectra

The normalized wave spectral energy density in the frequency–time frame is used to study the energy distribution of waves (Fig. 8). Each wave spectrum is normalized by the maximum wave spectral energy density of the respective spectrum. Left two panels of Fig. 8 shows the time series plot of the normalized spectral energy density with frequency in 2014 and 2015. The contour plots of normalized spectral energy density shows a very narrow spectrum within a short frequency range (0.05–0.15 Hz) in southwest monsoon, whereas during the non-monsoon period, much broader spectrum with two distinct peaks is observed (Fig. 8). In some days, a predominance of wind-seas having high frequency (0.2–0.3 Hz) is observed during December–May. Over an annual cycle, the majority of the data recorded are multi-peaked spectra (63%) and 80% of the multi-peaked spectra are swell dominated. Sanil Kumar et al. (2014) reported that for location 200 km southwest of the present study area, multi-peaked spectrum is with a narrow swell and a broader wind-sea.

To study the month to month variations in a year, the monthly average wave spectra for the year 2015 from the measured data is compared (Fig. 9). During June to September, two predominant swell systems are present in the study area, one at 0.1–0.12 Hz from 161 to 165° and the other at 0.065–0.07 Hz from 155 to 156°. The long-period swells (0.065–0.07 Hz) are result of the southerly swells and have maximum energy during June to September when the southern extra-tropical storm belt moves northwards. The

swells with period 0.1–0.12 Hz are due to the influence of the SW monsoon. The wave spectra observed is single-peaked during October and November and multi-peaked during the rest of the months. Single-peaked spectra during October–November are due to the impact of the more number of storm/cyclonic activities during these months in BoB, because of the low vertical wind shear compared to other months, which enhances cyclogenesis. During October, due to the impact of cyclones, the spectrum obtained is narrowest compared to other months. Only long period waves are observed in October and wind-seas are found to have maximum energy during April. In April, the swells are from 151° with peak at 0.07 Hz and the wind-seas are from 187°.

The directional wave spectra clearly show two peaks; swell peak and wind-sea peak, except in the southwest monsoon period (Fig. 10). During all the months, the swell peak is around 0.1 Hz, from the south, whereas the wind-sea peak frequency and direction varies from season to season. From February to April, the wind-sea direction is from the south, with a peak frequency greater than 0.2 Hz. The wind-sea energy observed during February and March is very low compared to April, due to the strengthening of the sea breeze in April. During May, wind-sea peak is observed to be merging with the swell peak as the swell energy increases during this period. From June to September only high energy swells are visible in the spectrum. During October–January, as the swell energy decreases, the wind-sea peak becomes more evident and its direction changes to east. It can be clearly seen that during January, the wind-seas are from the east, with a peak frequency above 0.2 Hz. The quantitative summary of the seasonal wave characteristics of the study area is presented in Fig. 11 in the form of seasonal average directional wave spectra (i.e., complete representation of wave directions, frequencies and energy density). During the pre-monsoon period, the two-wave systems present are distinct in the study area.

To study the dominance of wind-seas and swells during different years; monthly average wave spectrum from January to December for all the 3 years are compared (Fig. 12). Large inter-annual variations are observed in October due to the occurrence of TCs.

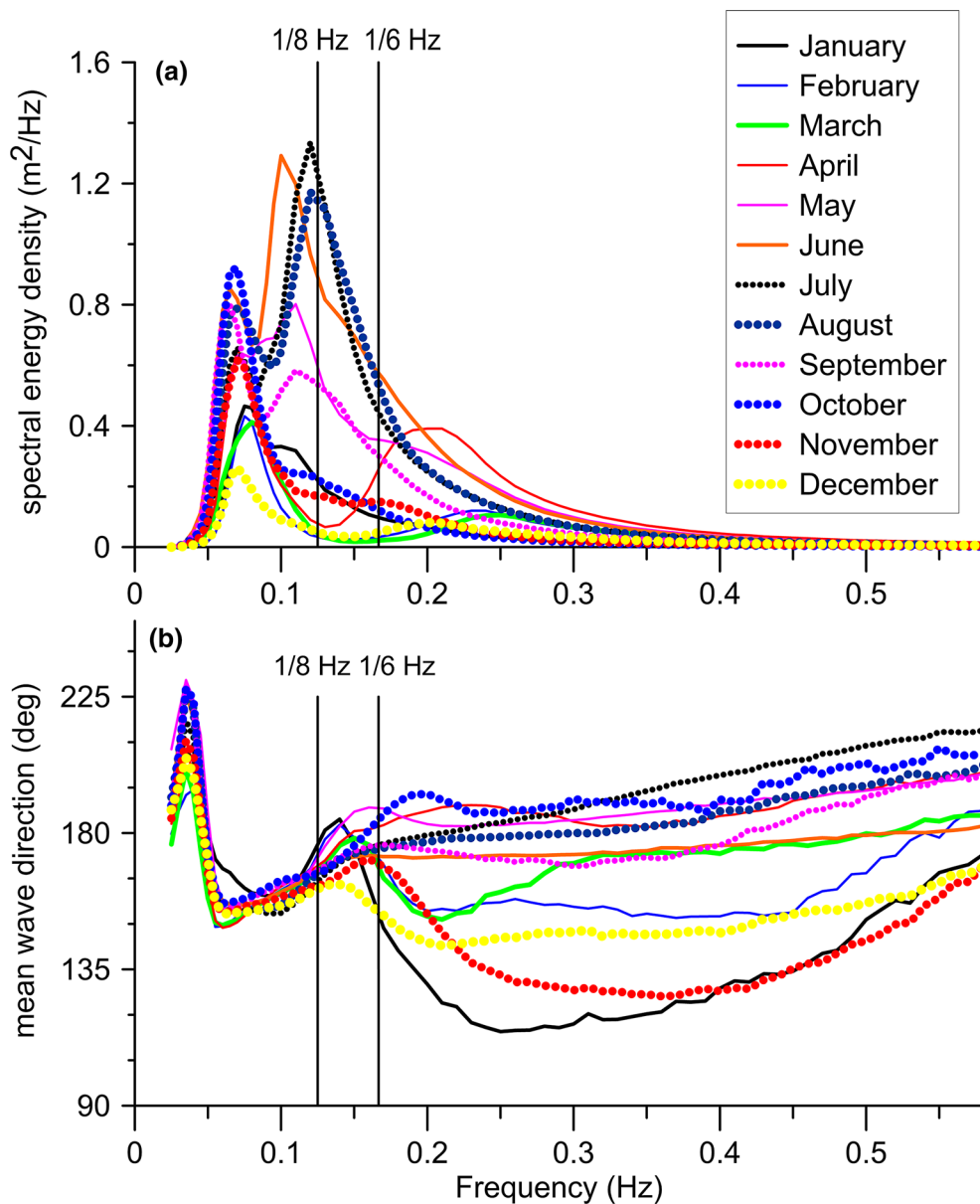


Figure 9

Monthly average wave spectrum (a) and mean wave direction (b) during January–December 2015 based on measured data spectral energy density (m²/Hz)

During the southwest monsoon time, a double-peaked spectrum is observed indicating the dominance of both wind-seas and swells, which is in contrast to the observations in the Arabian Sea, where single-peaked wave spectra are observed. In the southeastern BoB, Glejin et al. (2013) observed that the wave spectra during the southwest monsoon are multi-peaked,

whereas during the post-monsoon season wave spectra are single-peaked. In the study area, during June, July and August, the wind-sea peak observed have higher energy than the swell peak. The presence and variation of sea breeze over the east coast of India during the southwest monsoon period have been studied by Simpson et al. (2007) and found out that

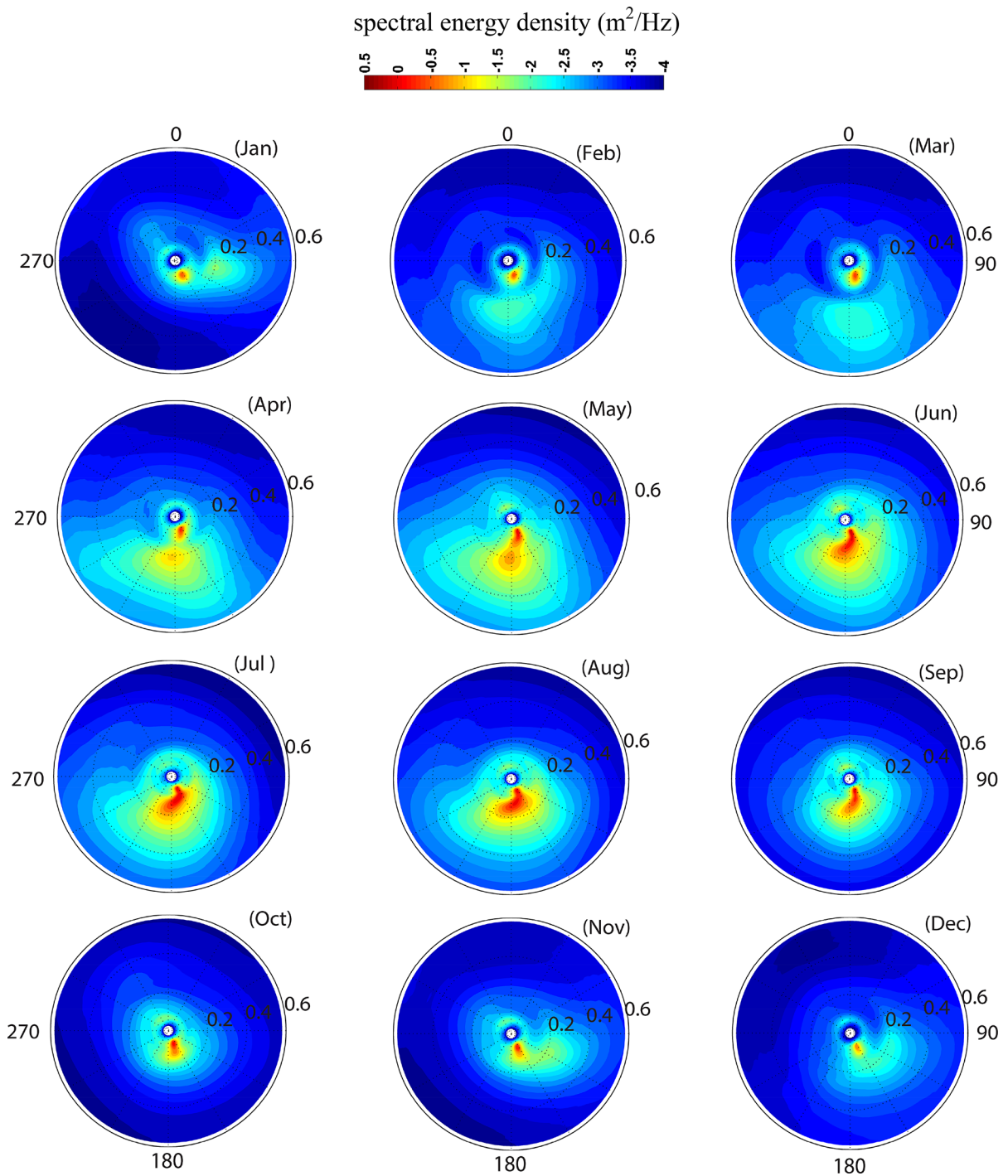


Figure 10
Monthly average wave directional spectrum in different months in 2015 based on measured data

sea breeze is most active during June followed by July and August. Maximum spectral energy density observed is during October 2013 ($> 4 \text{ m}^2/\text{Hz}$) due to

the influence of the cyclonic storm Phailin. Wind-sea peaks are between 0.2 and 0.4 Hz, showing the presence of much younger seas during former

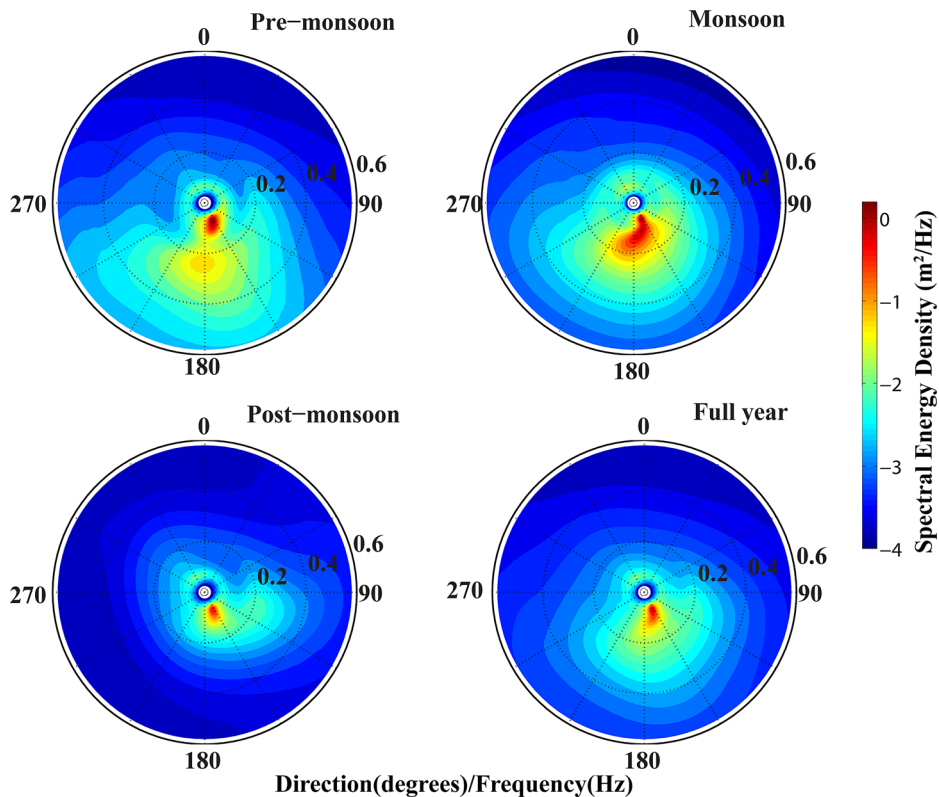


Figure 11

Seasonal average and annual average wave directional spectrum during the year 2015 based on measured data

months. Maximum wind-sea energy for the non-monsoon period is observed during April (2013 and 2015) from the south (Fig. 12) due to the influence of sea breeze. During the southwest monsoon period, maximum energy observed is during July 2013, due to the relatively stronger monsoon in 2013. Two right panels of Fig. 8 indicates the time series plot of wave direction with frequency. Wave spectra observed during May is specific, with multiple peaks because of the transition from NE to SW monsoon. During all the months, swells are observed from SSE direction ($140\text{--}180^\circ$) except in January 2013 and December 2013 (Fig. 13). During these 2 months, the spectrum observed is specific, with swells from SW and wind-seas from NW. Wind-seas are observed from SE during January to May and December.

Often, the wave direction and period of the largest energy peak of a spectrum is reported in the earlier studies (Mishra et al. 2011; Amrutha et al. 2014; Patra et al. 2016) and used in estimation of longshore

sediment transport, while the wave direction and the period of the secondary spectral peak, which has substantial energy is neglected in most of the studies. During the year 2015, the spectral energy density at secondary peak is 0.01–0.90 of the spectral energy density at primary peak with an average value of 0.41 (Fig. 14a). There is also large difference (up to 100°) between the wave direction at the primary peak and the secondary peak with a mean difference of 22° (Fig. 14b). When the spectral energy density at secondary peak is comparable to that at the primary peak, ignoring the wave direction of the secondary peak and using only the wave direction of the primary peak (which is the general practice) will lead to potentially misleading results of the longshore sediment transport (Sanil Kumar et al. 2000).

Diurnal changes in wave spectra show large variations in the wind-sea part (Fig. 15). It can be seen that the swell peak remains constant irrespective of time, whereas the wind-sea peak changes. The

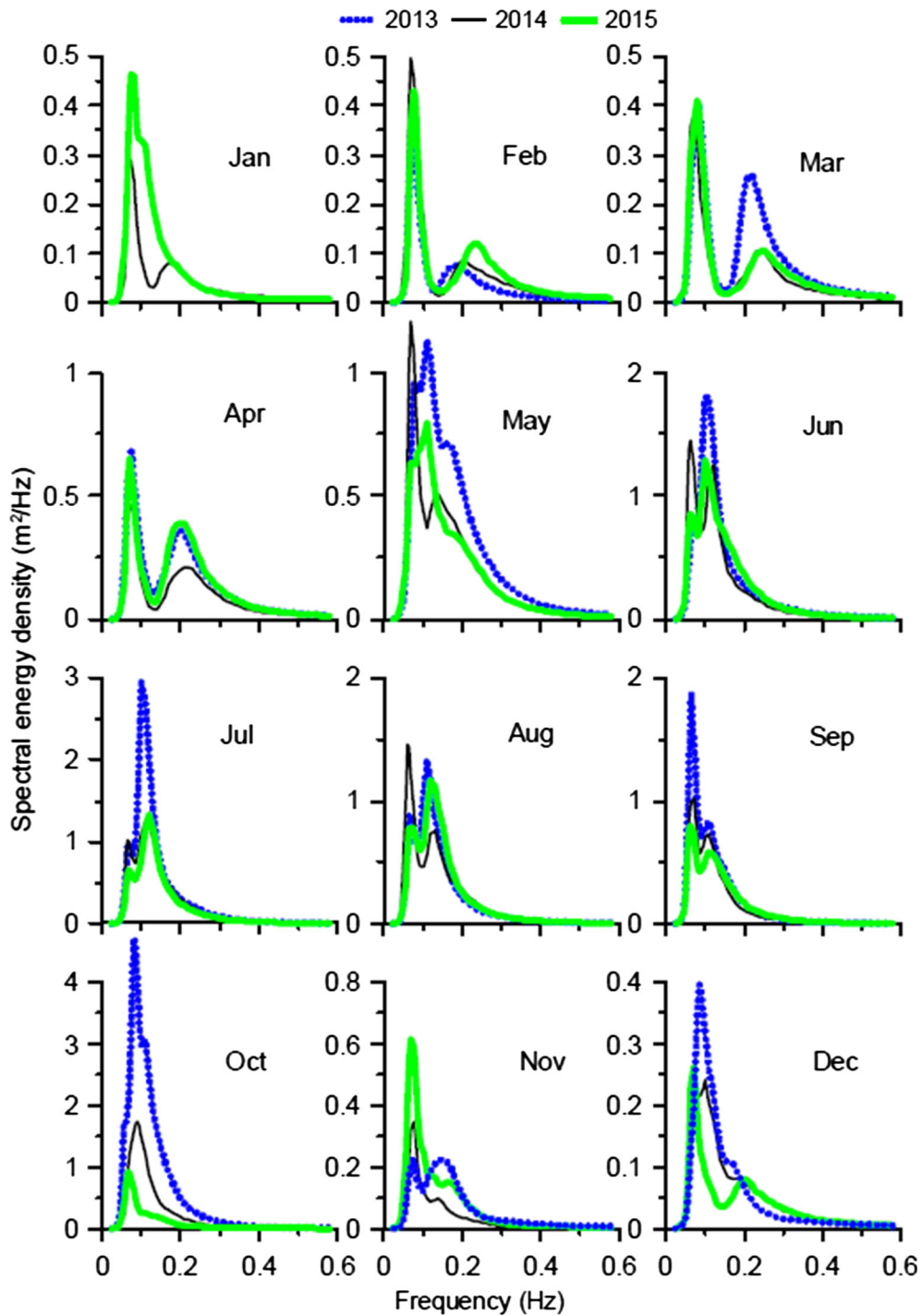


Figure 12
Monthly average wave spectrum during January–December in 2013, 2014 and 2015

changes in the wind-sea peak are more evident during February–April, since it is the fair-weather period and monsoon winds are absent, the effect of local winds

become dominant. During this period, the wind-sea energy gradually grows from 0 to 12 h, reaches its peak during 12 h and then decays.

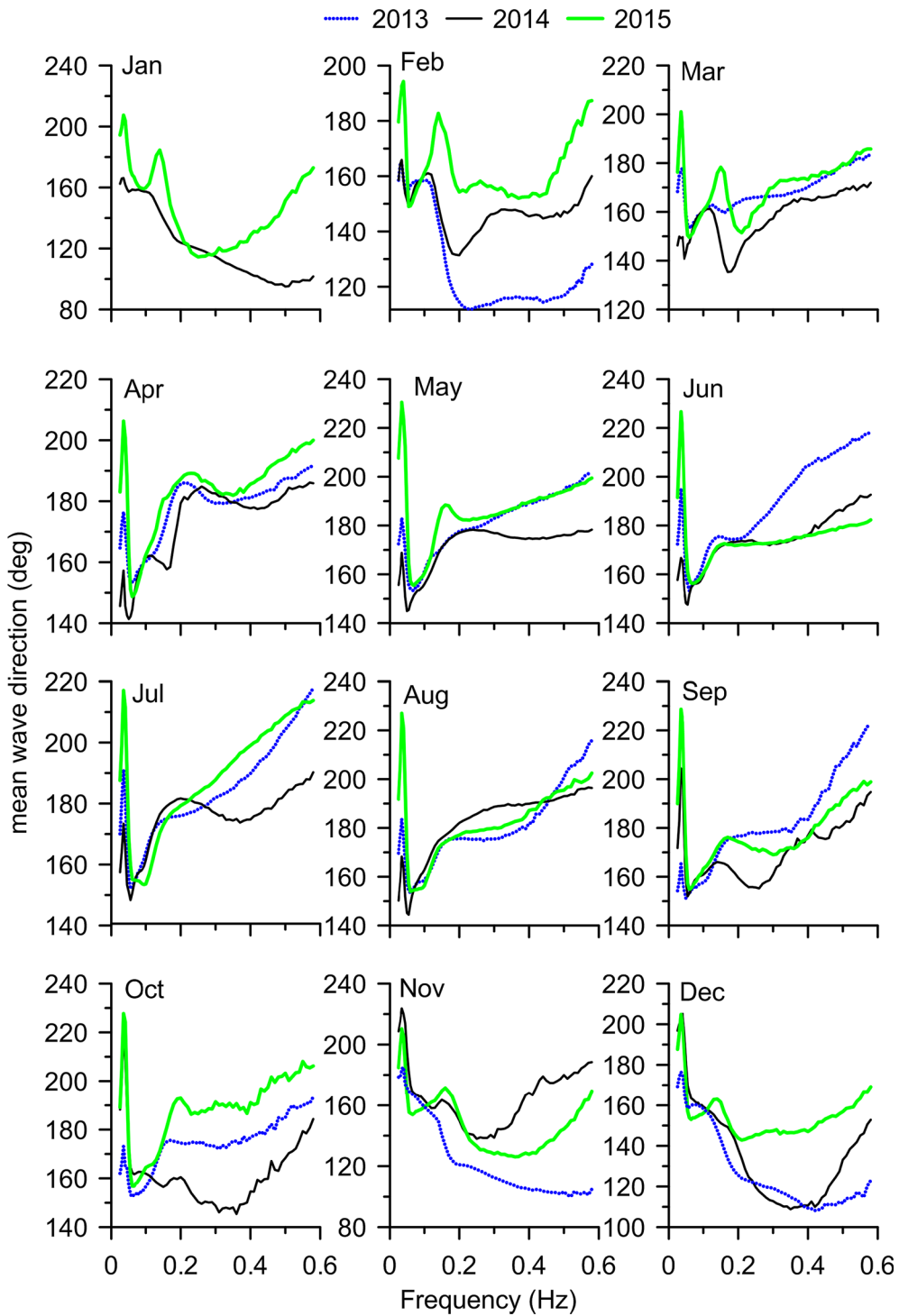


Figure 13
Monthly average wave direction during January–December in 2013, 2014 and 2015

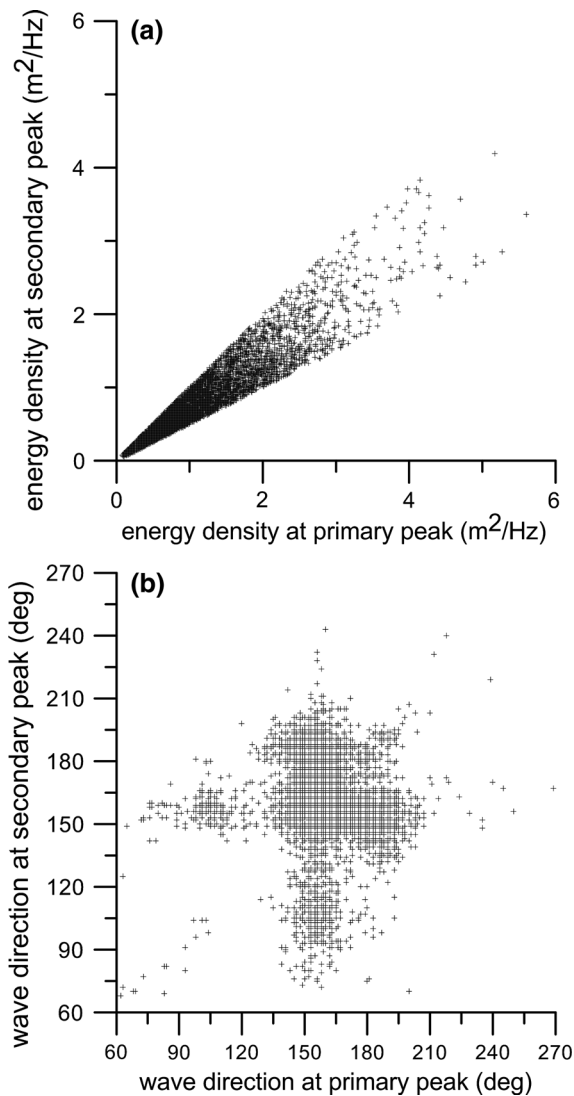


Figure 14

a Scatter plot of spectral energy density at primary peak and at secondary peak, **b** wave direction at primary peak and wave direction at secondary peak

The grouping of wave spectra based on the peak frequency indicates that during 51.5% of the time in an annual period, the frequencies between 0.06 and 0.08 Hz are predominant (Table 1). In a year during 11.7% of the time, wave spectra are with frequencies < 0.06 Hz. The wave spectra with peak frequency ranging from 0.06 to 0.10 Hz are single peaked (Fig. 16). Those with peak frequency ranging from 0.05 to 0.06 Hz and from 0.15 to 0.3 Hz are double-

peaked spectra. For spectra with peak frequency between 0.04 and 0.05 Hz, three peaks are observed, (i) the predominant peak at 0.05 Hz due to long period swell and another peak at 0.07 Hz due to swell and the third peak at 0.13 Hz due to the wind-sea. The grouping of all the wave spectra in 1 year based on the significant wave height indicates that high waves ($H_{m0} > 2$ m) are single-peaked wave spectra with the spectral peak at ~ 0.1 Hz and during 1.5% of the time waves are in this group (Fig. 17). For waves with H_{m0} between 1 and 2 m, the wave spectra are double peaked with peak frequencies at 0.065 and 0.118 Hz and 46% of the waves measured are under this category. The waves with $H_{m0} < 1$ m has peak frequencies at 0.072 and 0.247 Hz. Occurrence of single-peaked spectra are high (65.7%) during January compared to other months (Table 2). During June to August, the multi-peaked spectra are more (79.6–91.8%) compared to other months. During the 1-year period, single-peaked spectra are observed for 37.6% of time and the remaining are predominantly swell-dominated (49.9%) multi-peaked spectra and the wind-sea dominated multi-peaked spectra observed is only 6.6% (Table 2). Earlier studies indicate that the waves in the northwestern BoB consist of wind-seas and swells with the predominance of swells (Patra et al. 2016). Chen et al. (2002) observed that swell occurs more than 80% of the time in most of the world's oceans and wind waves occur most frequently in the mid-latitudes, decreasing to a minimum at the equator. Sanil Kumar et al. (2014) observed larger number of single-peaked spectra (56.8%) for location 200 km southwest of the present study area.

Since the coastal inclination is 48° to the east, the waves with angle more than 138° can create northerly longshore current. Hence, the waves are separated into three categories; (i) from 0 to 48° and from 228 to 360° , (ii) from 48 to 138° and (iii) 138 to 228° . One year data of 2015 shows that 75% of the surface height variance in a year is a result of waves from 138 to 228° , 17% are from 48 to 138° and balance 8% are from 0 to 48° and 228 to 360° . Significant percentage of waves from 48 to 138° is during November–February (Fig. 18). Compared to the easterly waves,

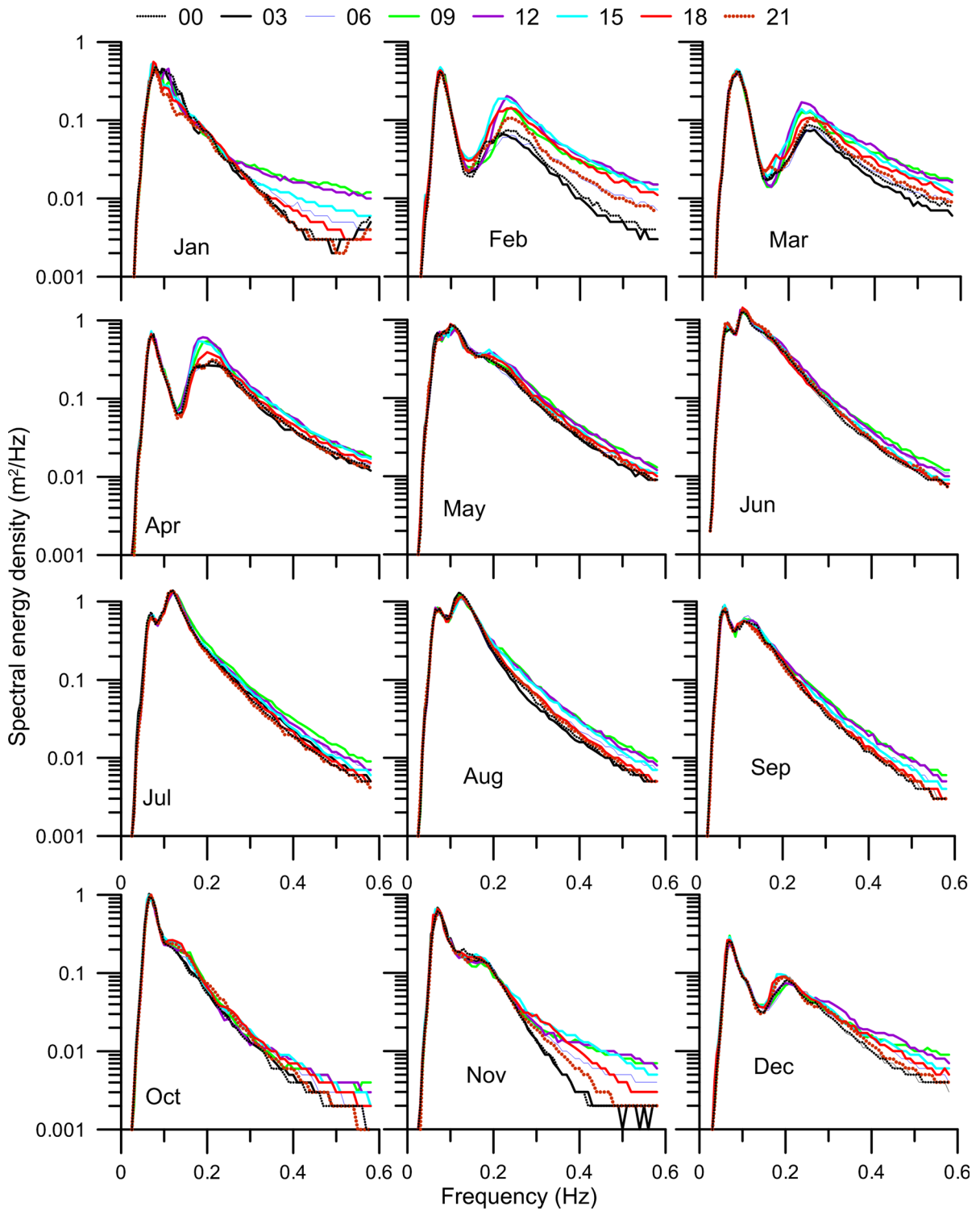


Figure 15
Monthly averaged wave spectra at different time in a day during January–December 2015 based on measured data

Table 1
Range of wave parameters for different spectral peak frequency

Peak frequency (f_p) range (Hz)	H_{m0} (m)	T_{m02} (s)	Mean wave direction (deg)	Peak wave period (s)	Data (%)
$0.04 < f_p \leq 0.05$	0.32–2.18 (1.19)	3.6–10.0 (6.4)	97–286 (155)	20–22.2 (20.1)	0.83
$0.05 < f_p \leq 0.06$	0.36–2.29 (1.10)	3.2–12.7 (6.5)	17–301 (155)	16.7–18.2 (17.1)	10.91
$0.06 < f_p \leq 0.07$	0.29–2.3 (0.93)	3.1–12.1 (6.1)	73–291 (156)	14.3–15.4 (14.8)	27.33
$0.07 < f_p \leq 0.08$	0.27–5.74 (0.78)	2.9–11.3 (5.8)	118–252 (158)	12.5–13.3 (13.0)	24.21
$0.08 < f_p \leq 0.10$	0.26–5.84 (0.94)	3.0–9.8 (5.7)	128–224 (159)	10–11.8 (11.1)	17.27
$0.10 < f_p \leq 0.15$	0.33–4.13 (1.43)	3.4–8.6 (6.0)	94–191 (163)	6.7–9.1 (8.2)	13.11
$0.15 < f_p \leq 0.2$	0.36–2.6 (1.12)	3.4–6.7 (4.6)	70–205 (153)	5–6.3 (5.6)	3.83
$0.2 < f_p \leq 0.5$	0.37–1.63 (0.96)	3.1–5.4 (3.8)	59–219 (176)	2.9–4.8 (4.4)	2.52

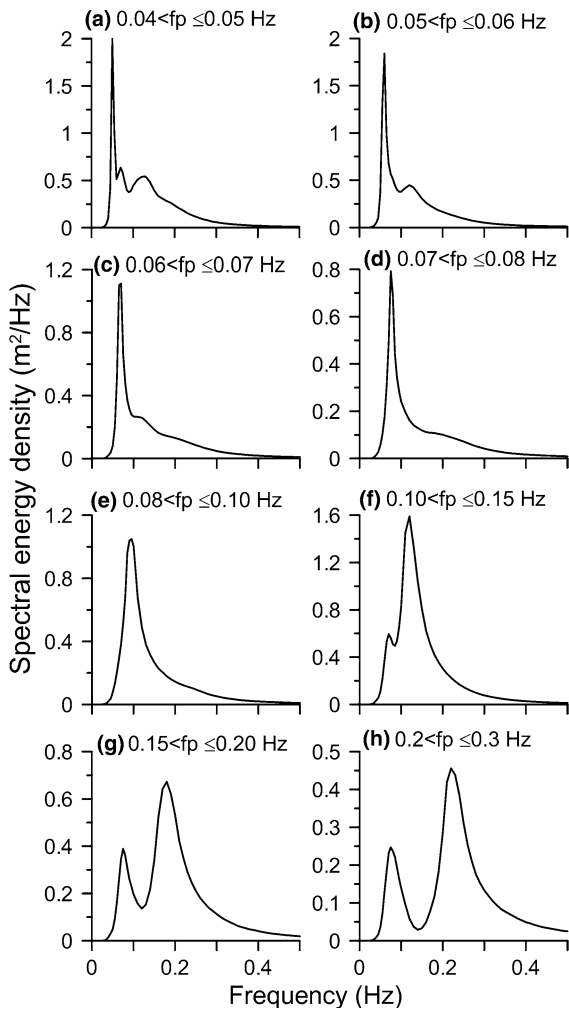


Figure 16
Average wave spectra for different peak frequency ranges

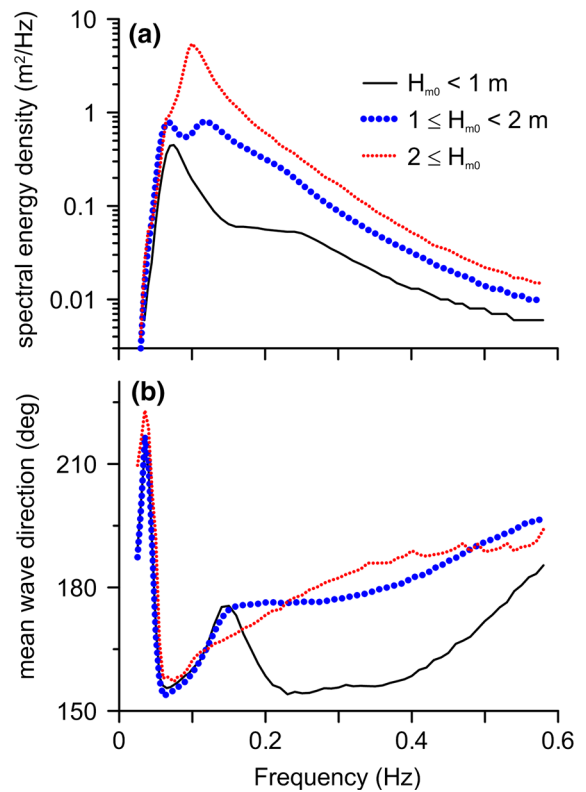


Figure 17
Plot of **a** average spectral energy density and **b** average mean wave direction of waves under different H_s with frequency in 2015

the south–southwesterly waves are more energetic (Fig. 18). The waves from 0 to 48° and from 228 to 360° are the waves approaching the buoy location from the coast. The wave from the coast are partly due to land breeze and partly the reflected waves

Table 2

Percentage of single-peaked- and multi-peaked wave spectra in different months in the year 2015 along with classification under wind-sea, swell or mixed based on spectral peak period

Months	Single-peak (%)				Multi-peak (%)			
	Total ($T_p < 6$)	Wind-sea ($T_p < 6$)	Swell ($T_p > 8$)	Mixed ($6 < T_p < 8$)	Total ($T_p < 6$)	Wind-sea dominated ($T_p < 6$)	Swell dominated ($T_p > 8$)	Mixed ($6 < T_p < 8$)
January	65.7	0.0	65.1	0.6	34.3	0.3	30.7	3.3
February	43.3	0.1	43.2	0.0	56.7	13.6	43.1	0.0
March	49.5	0.1	49.4	0.0	50.5	4.5	45.9	0.1
April	26.5	0.4	26.0	0.1	73.5	29.3	42.6	1.6
May	36.8	0.3	36.1	0.4	63.2	6.6	51.4	5.2
June	20.4	0.1	20.2	0.1	79.6	2.9	71.5	5.3
July	20.2	0.0	19.8	0.4	79.8	0.1	61.8	17.9
August	8.2	0.0	7.2	1.0	91.8	2.0	63.2	26.6
September	35.8	0.1	35.6	0.2	64.2	1.7	56.7	5.7
October	58.7	0.1	58.3	0.2	41.3	0.3	38.2	2.8
November	47.4	0.0	47.4	0.0	52.6	4.7	45.9	2.0
December	38.2	0.7	37.5	0.1	61.8	13.0	47.4	1.3
Annual average	37.6	0.1	37.2	0.3	62.4	6.6	49.9	6.0

(Anoop et al. 2014). A clear semi-diurnal variation is observed in the wave height and period of the waves from the coast (Fig. 19). The height of the waves from the coast is also found to vary with the tide. Since the measured wind data with a good temporal resolution is not available, further investigation on the influence of land breeze on the wave height is not attempted.

3.3. Long-Term Trend in Wave Height

Since the measured wave data is for a short-period, the long-term trends in mean H_{m0} are presented based on the ERA-I reanalysis datasets from 1979 to 2015 (Fig. 20). The annual mean H_{m0} is 1.28 m for 1979 to 2015 with a standard deviation of 0.34 m and it varied from 1.2 m (in 2015) to 1.34 m (in 2005). In the study area, a statistically insignificant weak decreasing trend ($-0.009 \text{ cm year}^{-1}$) in the annual mean H_{m0} is observed during 1979 to 2015. For the central BoB during 1979 to 2012,

Shanas and Sanil Kumar (2015) reported almost stable or no significant trend in annual mean H_{m0} . Aarnes et al. (2015) observed that during 1979–1991, there is an increase (0–0.5% of annual mean value per year) of H_{m0} in north Indian Ocean and from 1992 to 2012, there is a decrease (0–0.5% of annual mean value per year). Sanil Kumar and Anoop (2015) reported a weak decreasing trend (maximum $\sim -0.18 \text{ cm year}^{-1}$) in H_{m0} in the northwestern BoB during 1979–2012. Based on the altimeter data, Kumar et al. (2013) observed that the variation in SWH is almost negligible for a period of 18 years in the North Indian Ocean. Since the waves in the study area show strong seasonal changes, the trend during different seasons (i) February–May, (ii) June–September and (iii) October–January are also examined and presented in Fig. 20. The seasonal trend for June–September is increasing ($0.32 \text{ cm year}^{-1}$), whereas during the other two seasons, it is negative with larger negative values ($0.28 \text{ cm year}^{-1}$) during February–May.

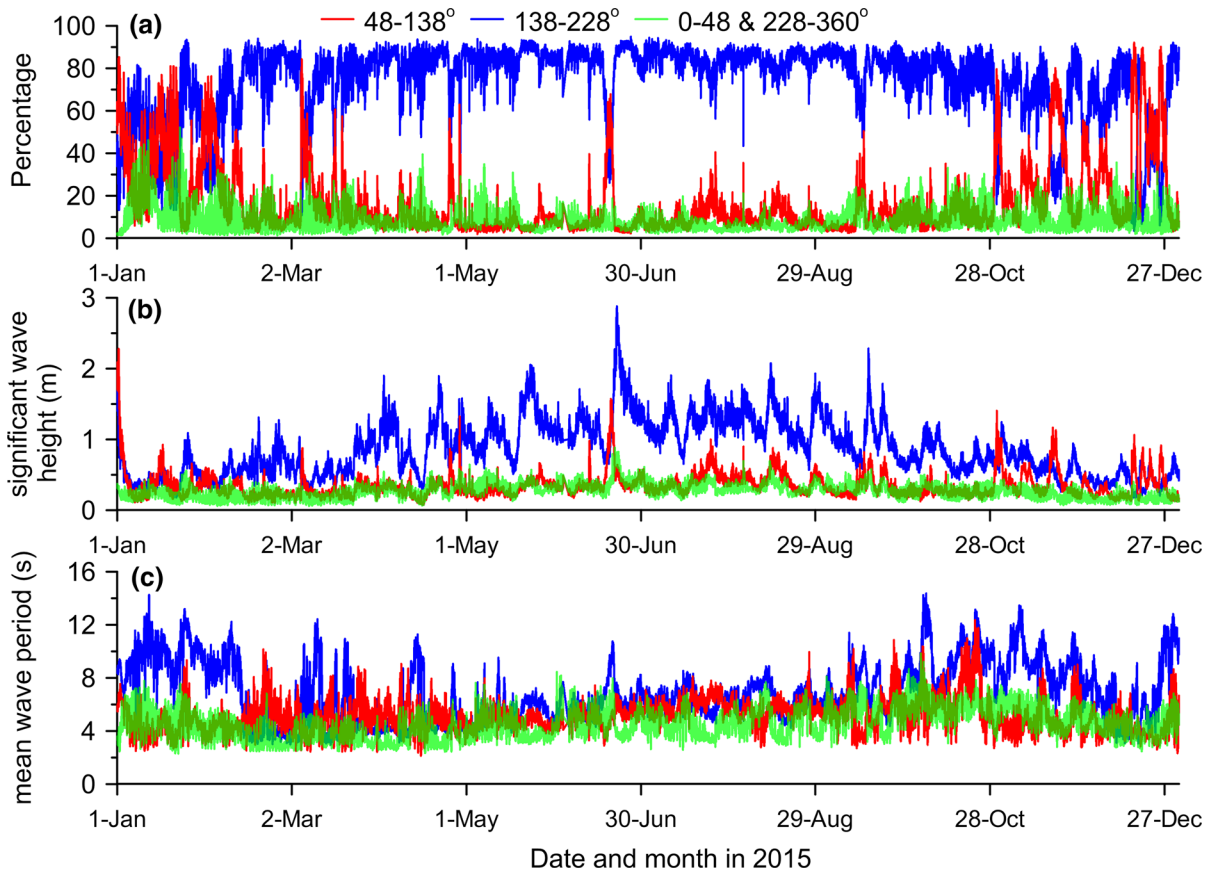


Figure 18

a Percentage of surface height variance from different directions ($0\text{--}48^\circ$ and $228\text{--}360^\circ$, $48\text{--}138^\circ$ and $138\text{--}228^\circ$), **b** corresponding significant wave height and **c** the mean wave period

4. Conclusions

The seasonal to the annual variability of the waves in the northwestern Bay of Bengal is analyzed using measured data by means of a directional waverider buoy. Results of this study show that the annual maximum significant wave height is significantly influenced by the tropical cyclone, whereas the change in annual mean value due to the tropical cyclone is not significant. The present study indicates that significant wave heights are usually < 2 m at this

location and waves are primarily (74%) from the southeast–southwest at $\sim 138\text{--}228^\circ$. A secondary easterly wave direction ($48\text{--}138^\circ$) are also seen. The measured data shows that the southerly and south-easterly swells control the wave regime in this region. During the southwest monsoon period, a double-peaked spectrum is observed indicating the dominance of both wind-seas and swells. During all the months, the swell peak is around 0.1 Hz, from the south–southeast, whereas the wind-sea peak frequency and direction varies from season to season.

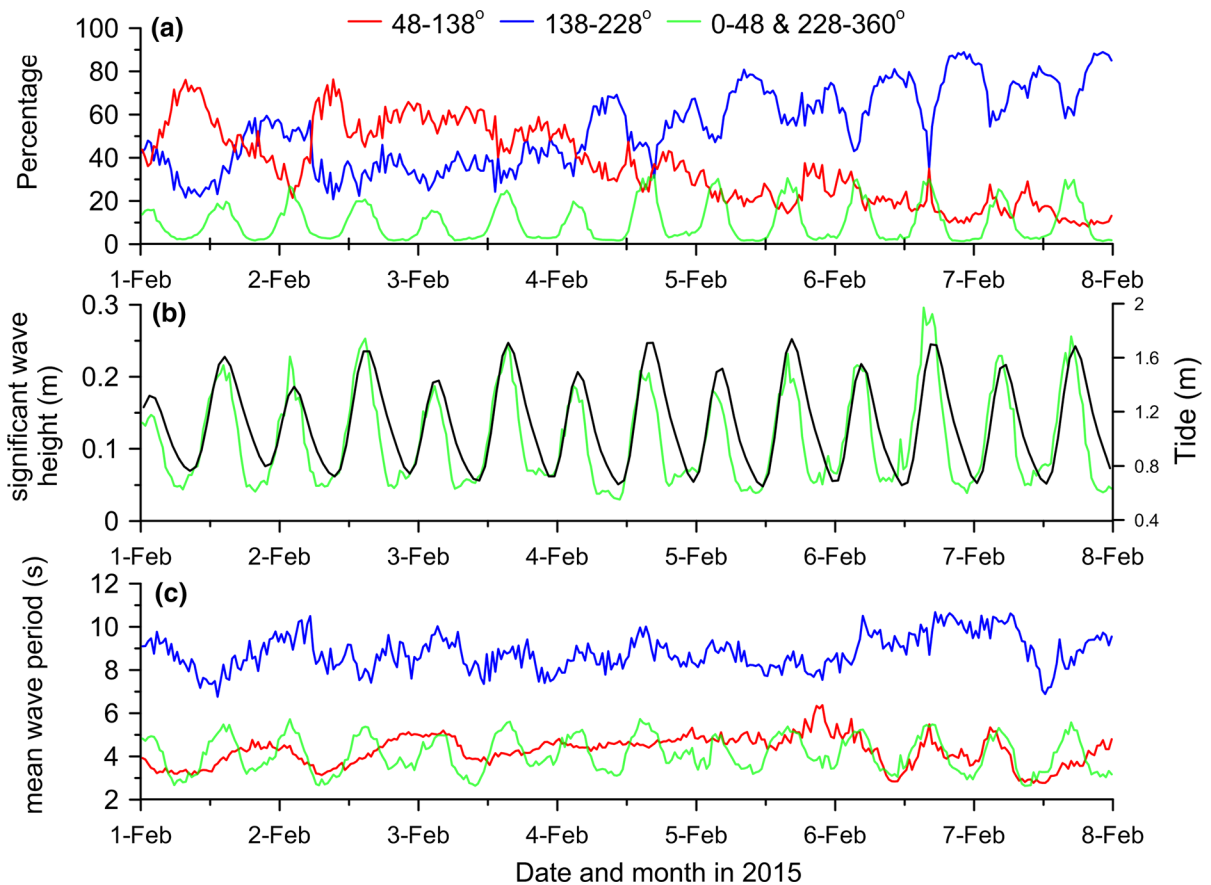


Figure 19

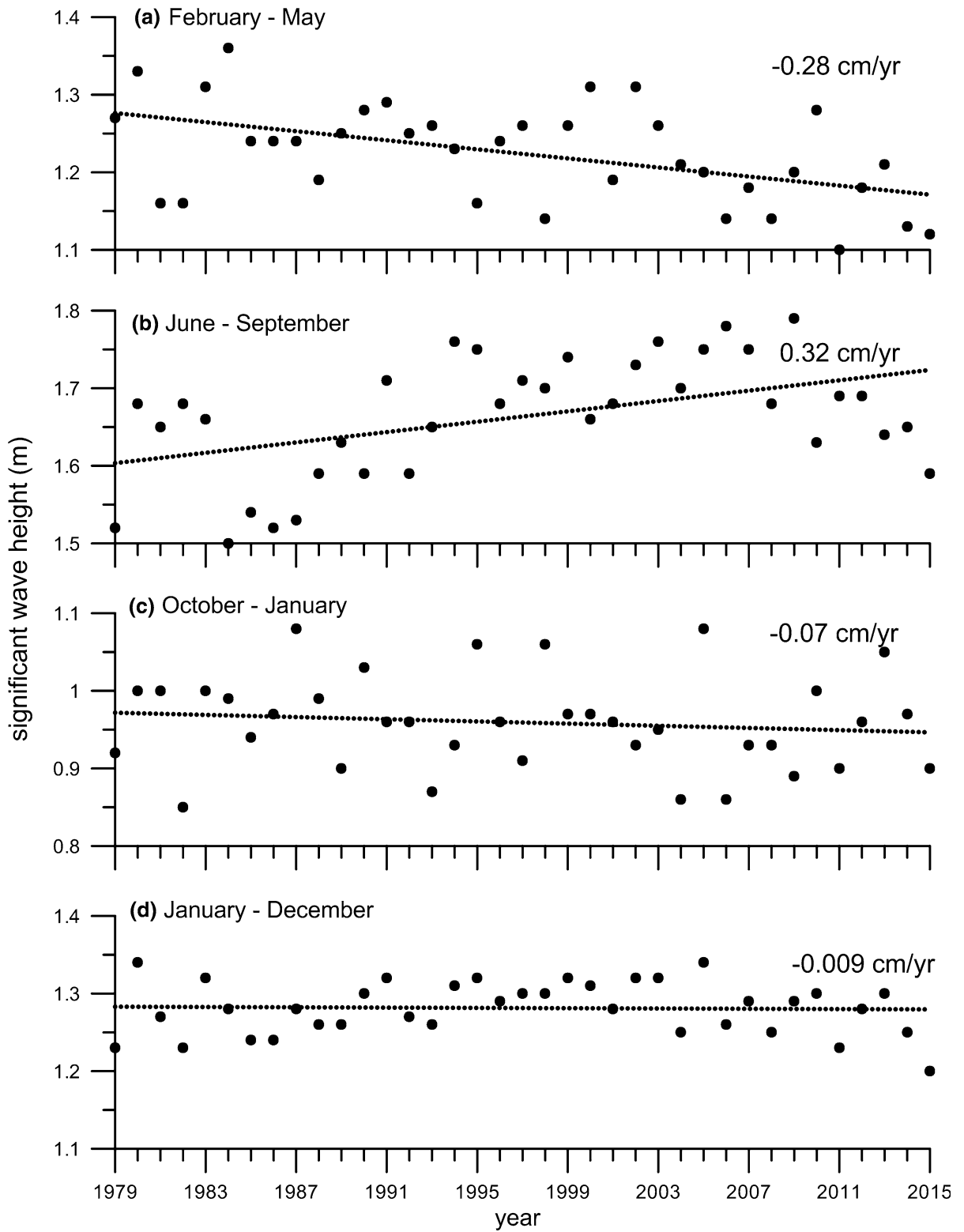
a Percentage of surface height variance from different directions (0–48° and 228–360°, 48–138° and 138–228°), **b** corresponding significant wave height and tide, **c** the mean wave period during 1–8 February 2015. Black line in (b) is tide

Around half of the time in a year, the wave spectral peak is predominantly between 0.06 and 0.08 Hz.

Acknowledgements

The authors gratefully acknowledge the financial support given by the Council of Scientific and Industrial Research, New Delhi and the Earth System Science Organization, Ministry of Earth Sciences, Government of

India to conduct this research work. We thank Dr. T. M. Balakrishnan Nair, Mr. Arun Nherakkol, Scientist, INCOIS and NIO colleague Mr. Jai Singh for the help during data collection. Chilka Development Authority, Bhubaneswar provided the logistics during data collection period. The NCEP/NCAR wind data are provided by the NOAA-CIRES Climate Diagnostics Center, Boulder, Colorado at <http://www.cdc.noaa.gov/>. We thank both the reviewers for their critical comments and the suggestions. This article is CSIR-NIO contribution No.



◀Figure 20

Time series plot of seasonal average and annual average significant wave height during 1979–2015 based on ERA-I data. **a** Fair-weather period (February–March), **b** southwest monsoon (June–September), **c** post-monsoon (October–January) and **d** January–December

6187 and forms part of the Ph.D. Thesis of the first author.

REFERENCES

- Aarnes, O. J., Abdalla, S., Bidlot, J., & Breivik, O. (2015). Marine wind and wave height trends at different ERA-interim forecast ranges. *J. Climate*, 28, 819–837.
- Alam, M., Hossain, A., & Shafee, S. (2003). Frequency of Bay of Bengal cyclonic storms and depressions crossing different coastal zones. *International Journal of Climatology*, 23, 1119–1125.
- Amrutha, M. M., Sanil Kumar, V., Anoop, T. R., Balakrishnan Nair, T. M., Nherakkol, A., & Jeyakumar, C. (2014). Waves off Gopalpur, northern Bay of Bengal during Cyclone Phailin. *Annales Geophysicae*, 32, 1073–1083.
- Amrutha, M. M., Sanil Kumar, V., & George, Jesbin. (2017). Observations of long-period waves in the nearshore waters of central west coast of India during the fall inter-monsoon period. *Ocean Engineering*, 131, 244–262. <https://doi.org/10.1016/j.oceaneng.2017.01.014>.
- Anoop, T. R., Sanil Kumar, V., & Glejin, Johnson. (2014). A study on reflection pattern of swells from the shoreline of peninsular India. *Natural Hazards*, 74, 1863–1879.
- Anoop, T. R., Sanil Kumar, V., Shanass, P. R., & Johnson, G. (2015). surface wave climatology and its variability in the north Indian ocean based on ERA-Interim reanalysis. *Journal of Atmospheric and Oceanic Technology*, 32(7), 1372–1385.
- Balaguru, K., Taraphdar, S., Leung, L. R., & Foltz, R. R. (2014). Increase in the intensity of post monsoon Bay of Bengal tropical cyclones. *Geophysical Research Letters*, 41(10), 3594–3601.
- Chandramohan, P., Sanil Kumar, V., & Nayak, B. U. (1993). Coastal processes along the shorefront of Chilka lake. *Indian Journal of Marine Sciences*, 22, 268–272.
- Chen, G., Chapron, B., Ezraty, R., & Vandemark, D. (2002). A global view of swell and wind sea climate in the ocean by satellite altimeter and scatterometer. *Journal of Atmospheric and Oceanic Technology*, 19(11), 1849–1859.
- Datawell. (2009). *Datawell waverider reference manual* (p. 123). The Netherlands: Datawell BV Oceanographic Instruments.
- Dee, D. P., Uppala, S. M., Simmons, A. J., Berrisford, P., Poli, P., Kobayashi, S., et al. (2011). The ERA-Interim reanalysis: Configuration and performance of the data assimilation system: The ERA-Interim reanalysis: Configuration and performance of the data assimilation system. *Quarterly Journal of the Royal Meteorological Society*, 137, 553–597.
- Glejin, J., Sanil Kumar, V., & Nair, T. M. B. (2013). Monsoon and cyclone induced wave climate over the near shore waters off Puduchery, south western Bay of Bengal. *Ocean Engineering*, 72, 277–286.
- Hanson, J. L., & Phillips, O. M. (1999). Wind sea growth and dissipation in the open ocean. *Journal of Physical Oceanography*, 29(8), 1633–1648.
- Harikumar, R., Balakrishnan Nair, T. M., Rao, B. M., Rajendra Prasad, P., Ramakrishna Phani, C., Nagaraju, M., et al. (2016). Ground-zero met-ocean observations and attenuation of wind energy during cyclonic storm Hudhud. *Current Science*, 110, 2245–2252.
- Kuik, A. J., Van Vledder, G. P., & Holthuijsen, L. H. (1988). A method for the routine analysis of pitch-and-roll buoy wave data. *Journal of Physical Oceanography*, 18(7), 1020–1034.
- Kumar, D., Sannasiraj, S. A., Sundar, V., & Polnikov, V. G. (2013). Wind-wave characteristics and climate variability in the Indian ocean region using altimeter data. *Marine Geodesy*, 36, 303–313.
- Li, Z., Yu, W., Li, T., Murty, V. S. N., & Tangang, F. (2013). Bimodal character of cyclone climatology in the Bay of Bengal modulated by monsoon seasonal cycle. *Journal of Climate*, 26, 1033–1046.
- Mishra, P., Patra, S. K., Ramana Murthy, M. V., Mohanty, P. K., & Panda, U. S. (2011). Interaction of monsoonal wave, current and tide near Gopalpur, east coast of India and their impact on beach profile; a case study. *Natural Hazards*, 59(2), 1145–1159.
- Patra, S. K., Mishra, P., Mohanty, P. K., Pradhan, U. K., Panda, U. S., Ramana Murthy, M. V., et al. (2016). Cyclone and monsoonal wave characteristics of northwestern Bay of Bengal: long-term observations and modeling. *Natural Hazards*, 82, 1051–1073.
- Portilla, J., Ocampo-Torres, F. J., & Monbaliu, J. (2009). Spectral partitioning and identification of wind-sea and swell. *Journal of Atmospheric and Oceanic Technology*, 26, 117–122.
- Sanil Kumar, V., Chandramohan, P., Ashok Kumar, K., Gowthaman, R., & Pednekar, P. (2000). Longshore currents and sediment transport along Kannirajapuram coast. *Tamilnadu, India, Journal of Coastal Research*, 16(2), 247–254.
- Sanil Kumar, V., Anand, N. M., Kumar, K. A., & Mandal, S. (2003). Multi peakedness and groupiness of shallow water waves along Indian coast. *Journal of Coastal Research*, 19, 1052–1065.
- Sanil Kumar, V., & Anoop, T. R. (2015). Spatial and temporal variations of wave height in shelf seas around India. *Natural Hazards*, 78, 1693–1706.
- Sanil Kumar, V., Dubhashi, K. K., & Nair, T. B. (2014). Spectral wave characteristics off Gangavaram, Bay of Bengal. *Journal of Oceanography*, 70(3), 307–321.
- Shanass, P. R., & Sanil Kumar, V. (2015). Trends in surface wind speed and significant wave height as revealed by ERA-Interim wind wave hindcast in the Central Bay of Bengal. *International Journal of Climatology*, 35, 2654–2663.
- Simpson, M., Warrior, H., Raman, S., Aswathanarayana, P. A., Mohanty, U. C., & Suresh, R. (2007). Sea-breeze-initiated rainfall over the east coast of India during the Indian southwest monsoon. *Natural Hazards*, 42(2), 401–413.
- Soares, C. G. (1991). On the occurrence of double peaked wave spectra. *Ocean Engineering*, 18(1–2), 167–171.
- Suresh, R. V., Annapurnaiah, K., Reddy, K. G., Lakshmi, T. N., & Balakrishnan Nair, T. M. (2010). Wind sea and swell characteristics off east coast of India during southwest monsoon. *International Journal of Oceans and Oceanography*, 4(1), 35–44.
- Thadathil, P., Muraleedharan, P. M., Rao, R. R., Somayajulu, Y. K., Reddy, G. V., & Revichandran, C. (2007). Observed seasonal

variability of barrier layer in the Bay of Bengal. *Journal of Geophysical Research*, 112, C02009.

Wang, S. Y., Buckley, B. M., Yoon, J. H., & Fosu, B. (2013). Intensification of premonsoon tropical cyclones in the Bay of

Bengal and its impacts on Myanmar. *Journal of Geophysical Research*, 118(10), 4373–4384.

(Received October 18, 2017, revised March 6, 2018, accepted March 10, 2018, Published online March 17, 2018)